Electronic Supplementary Material (ESI) for Journal of Materials Chemistry A.

Supplementary Information

Study of the Electro-Oxidation of Borohydride on Directly Formed CoB/Ni-foam Electrode and Its Application in Membraneless Direct Borohydride Fuel Cells

Siqi Guo [a], Jie Sun [a], Zhengyan Zhang [a], Aokai Sheng [a], Ming Gao [a], Zhibin Wang [b], Bin Zhao [a,], Weiping Ding [a]*

[a] Key Laboratory of Mesoscopic Chemistry of MOE, School of Chemistry and Chemical Engineering, Nanjing University, Nanjing 210046, PR China

[b] State Key Laboratory of Coordination Chemistry, School of Chemistry and Chemical Engineering, Nanjing University, Nanjing 210046, PR China

* To whom correspondence should be addressed.

E-mail: binzhao@nju.edu.cn

SAED analysis

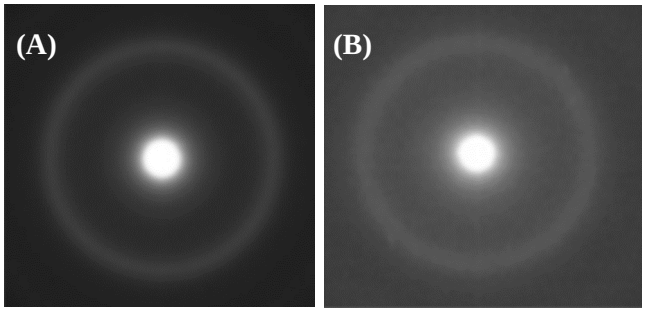

Fig. S1 The SAED patterns of CoB particles in (A) CoB/Ni-foam (7EP) and (B) CoB plate

The SEAD tests were performed to clarify the structure of CoB in CoB/Ni-foam (7EP) and CoB plate, the results were shown in Fig. S1. Both the patterns demonstrated dispersive ring which indicated non-crystalline nature of CoB and the results were in good accordance with the Lu's work.[1]

Note: Because of the high stability of CoB/Ni-foam, the CoB in CoB/Ni-foam (7EP) could only be detached from the Ni-foam substrate by sonicating it in deoxygenated water for 1 hour.

The method for analyzing the active surface areas of CoB/Ni-foam

The active surface areas of CoB/Ni-foam (or CoB plate) were evaluated by scanning CVs in a solution with redox couple of $K_3[Fe(CN)_6]$ and $K_4[Fe(CN)_6]$ and calculated according to Randles – Sevcik equation:[2]

$$i_p = 0.4463\times10^{-3}n^{3/2}F^{3/2}A(RT)^{-1/2}D_R^{1/2}C_Rv^{1/2} \qquad (1)$$

where i_p was the peak current (A), n was the number of electron transferred (for $K_3[Fe(CN)_6]$ / $K_4[Fe(CN)_6]$, n = 1), F was the Faraday constant (96485 C mol^{-1}), C_R was the concentration of $K_4[Fe(CN)_6]$ (mol L^{-1}), D_R was the diffusion coefficient of $K_4[Fe(CN)_6]$ (3.7×10^{-6} cm^2 s^{-1}), v was the scan rate (V s^{-1}) and A was the active surface area (cm^2). Because of the instability of CoB in $K_4[Fe(CN)_6]$ solution, only the active surface area of Ni-foam substrate could be measured by this method and the result was 0.355 cm^2.

It was also known that the double layer capacitance was proportional to the active surface area.[3-5] Hence, the active surface areas of the CoB/Ni-foam catalysts could be calculated according to the following equation:

$$\frac{A_{\text{Ni-foam}}}{A_{\text{CoB/Ni-foam}}} = \frac{C_{\text{Ni-foam}}}{C_{\text{CoB/Ni-foam}}} \qquad (2)$$

Where $C_{\text{Ni-foam}}$ and $C_{\text{CoB/Ni-foam}}$ were the double layer capacitances of Ni-foam substrate and CoB/Ni-foam, respectively. $A_{\text{Ni-foam}}$ and $A_{\text{CoB/Ni-foam}}$ were the active surface areas of Ni-foam substrate and CoB/Ni-foam, respectively.

The double layer capacitances of the catalysts could be estimated in N_2 saturated 2 mol L^{-1} KOH solution at a scan rate of 0.05 V s^{-1} in the potential range of − 0.4V to − 0.35 V vs. Hg/HgO according to the following equation:[6]

$$C = \frac{\int I\mathrm{d}V}{v\Delta V} \qquad (3)$$

where v was the scan rate (V s^{-1}), ΔV was the potential range (V), and $\int I\mathrm{d}V$ was the charge of double layer.

XPS analysis

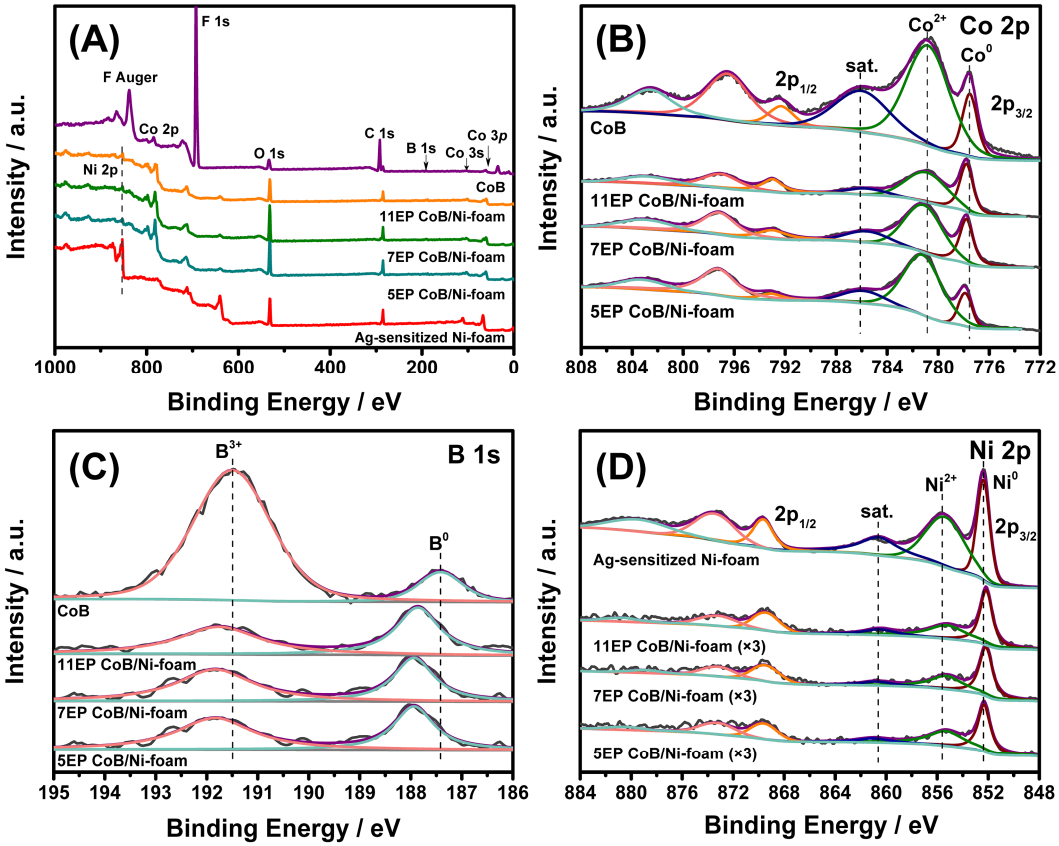

Fig. S2 XPS spectra of the Ag-sensitized Ni-foam, CoB/Ni-foam, CoB catalysts: (A) the survey spectra and the high resolution spectra for (B) Co 2*p*, (C) B 1*s* and (D) Ni 2*p*

XPS was performed to further investigate the surface existing states and the compositions of CoB/Ni-foam and CoB plate catalysts. The survey spectra of CoB/Ni-foam and CoB plate were shown in Fig. S2 (A). The existence of O was attributed to the surface oxidation during the XPS analysis. The surface composition and binding energy of each element were summarized in Table S1. The surface concentrations of Co for CoB/Ni-foam catalysts were much higher than that of CoB plate indicated the severe coverage of CoB by PTFE in CoB plate which was confirmed by the high surface concentration of F. Co was regarded as the active species for BH_4^- oxidation reaction, and the lower surface concentration of Co for CoB plate could account for its low catalytic activity. The Co $2p_{3/2}$ bands of CoB/Ni-foam and CoB plate (Fig. S2 (B)) could be deconvoluted into three bands, corresponding to Co^0, Co^{2+} and satellite peak respectively and all the catalysts showed similar binding energy of Co^0. The high resolution B 1*s* spectra were shown in Fig. S2 (C), the binding energy of B^0 for CoB/Ni-foam catalysts and CoB plate were higher than the literature (187.1 eV) [7,8] which was attributed to the electron-donating effects from B^0 to Co^0. Interestingly, the binding energy of B^0 in CoB/Ni-foam catalysts were about 0.3 eV higher than that of CoB plate which might be due to the further electron transfer from B^0 to Ni^0. The high-resolution of spectra Ni 2*p* were shown in Fig. S2 (D). As expected, the binding energy of Ni^0 for CoB/Ni-foam catalysts decreased compared to the Ag-sensitized Ni-foam substrate which confirmed the electron transfer between B^0 and Ni^0. Based on the XPS results, it could be clearly seen that there was a strong interaction between CoB and Ni-foam substrate in the directly formed CoB/Ni-foam catalysts prepared by electroless plating method which gave them a nice all-around performance boost.

Study the cyclic voltammetry (CV) in NaOH solution

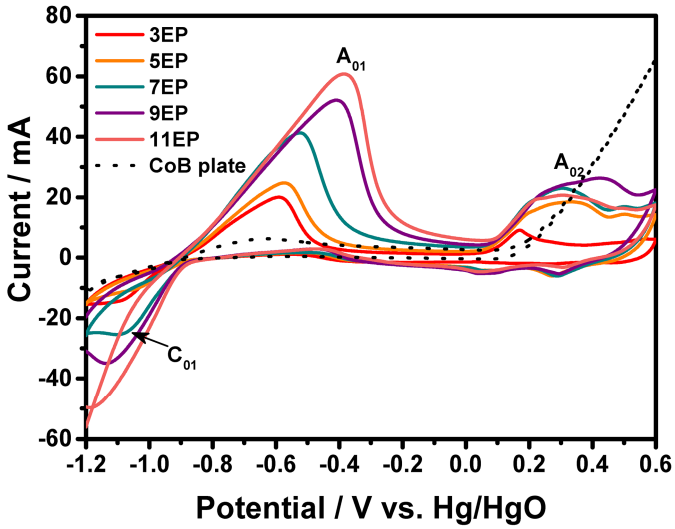

Fig. S3 Cyclic voltammograms of CoB/Ni-foam catalysts and CoB plate in N_2-saturated 3 mol L^{-1} NaOH solution (at scan rate of 50 mV s^{-1} at 298 K)

Fig. S3 showed the cyclic voltammograms of CoB/Ni-foam and CoB plate in a potential range of − 1.2 V to 0.6 V vs. Hg/HgO at a scan rate of 50 mV s^{-1} in 3 mol L^{-1} N_2 saturated NaOH solution. All the CoB/Ni-foam catalysts with different plating times showed similar electrochemical behaviors which were typical irreversible electrochemical process and in good accordance with the work reported by Y. Liu.[9] During the positive potential sweep, it could be clearly seen that a wide oxidation peak denoted as A_{01} appeared between − 0.9 V and 0.1 V vs. Hg/HgO which was attributed to the electrooxidation of CoB alloy to $Co(OH)_2$.[9] Corresponding to peak A_{01}, the reduction peak denoted as C_{01} in negative scanning process was attributed to the reduction of $Co(OH)_2$.[10] In addition, there were several anodic peaks emerged in the high potential range of positive scanning process (denoted as A_{02}). These peaks were attributed to the oxidation of Co to higher oxidation states step by step according to the following reactions [11]:

$$3\ Co(OH)_2 + 2\ OH^- \rightarrow Co_3O_4 + 4\ H_2O + 2\ e^- \qquad E^{\Theta} = -0.192V \text{ vs. Hg/HgO} \quad (4)$$

$$Co(OH)_2 + OH^- \rightarrow CoOOH + H_2O + e^- \qquad E^{\Theta} = -0.054V \text{ vs. Hg/HgO} \quad (5)$$

$$Co_3O_4 + 4\ OH^- \rightarrow 3CoO_2 + 2\ H_2O + 4\ e^- \qquad E^{\Theta} = +0.477V \text{ vs. Hg/HgO} \quad (6)$$

$$CoOOH + OH^- \rightarrow CoO_2 + H_2O + e^- \qquad E^{\Theta} = +0.562V \text{ vs. Hg/HgO} \quad (7)$$

The beginning of peak A_{02} was about + 0.1V vs. Hg/HgO. Compared to the thermodynamically calculated value (E^{Θ}) of – 0.192V mentioned above, the positive potential shift indicated that there was an big overpotential involved in the oxidation of $Co(OH)_2$ to Co_3O_4 or might be attributed to existence of B in CoB alloy. As shown in Fig. S3, the currents of peak A_{01} and A_{02} increased with the plating times which accorded well with the CoB loading amount, XRD and SEM analysis results.

Study BOR activity by linear sweep voltammetry (LSV)

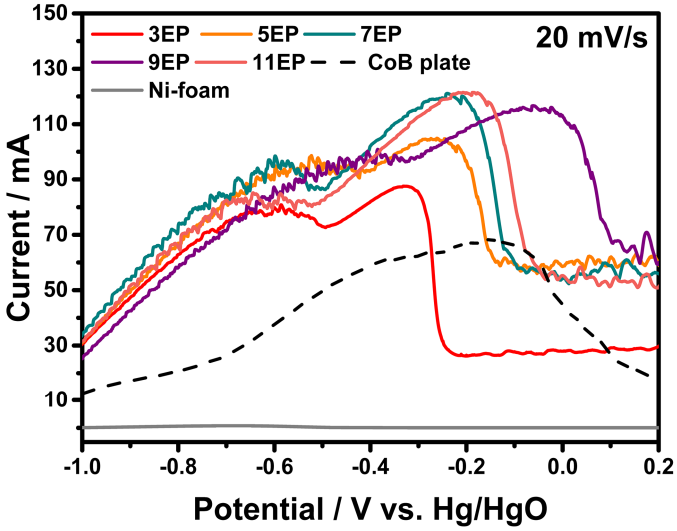

Fig. S4 Linear sweep voltammograms of CoB/Ni-foam catalysts with different electroless plating times in N_2-saturated 0.05 mol L^{-1} $NaBH_4$ + 3 mol L^{-1} NaOH solution with scan rate of 20 mV/s at 298 K

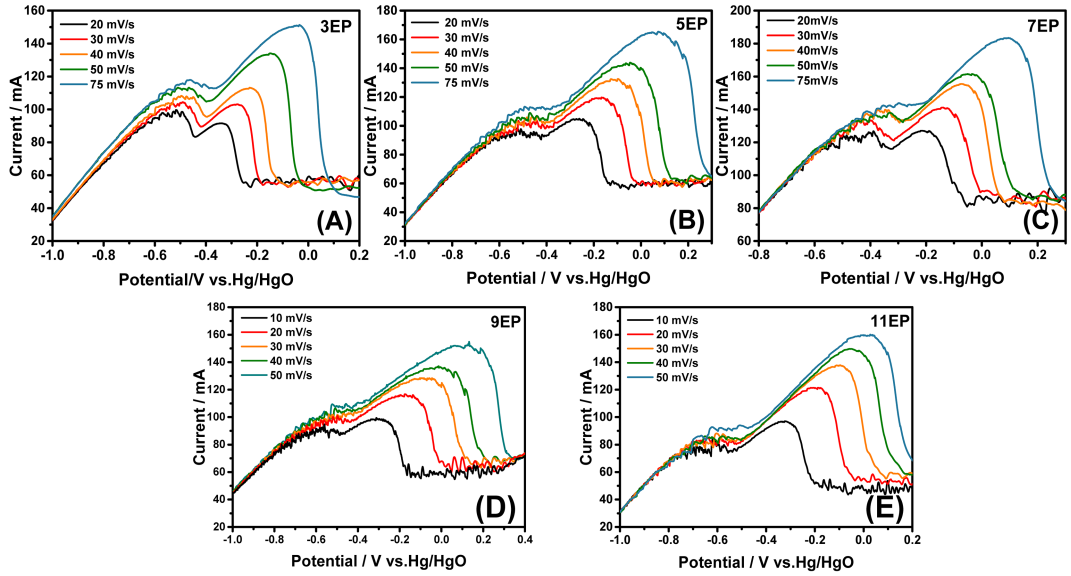

Fig. S5 Linear sweep voltammograms of CoB/Ni-foam catalysts with different electroless plating times in N_2-saturated 0.05 mol L^{-1} $NaBH_4$ + 3 mol L^{-1} NaOH solution with different scan rates at 298 K

The relationship of E_p with log$v$ and I_p with $v^{1/2}$ (for calculating electron transferred number of n)

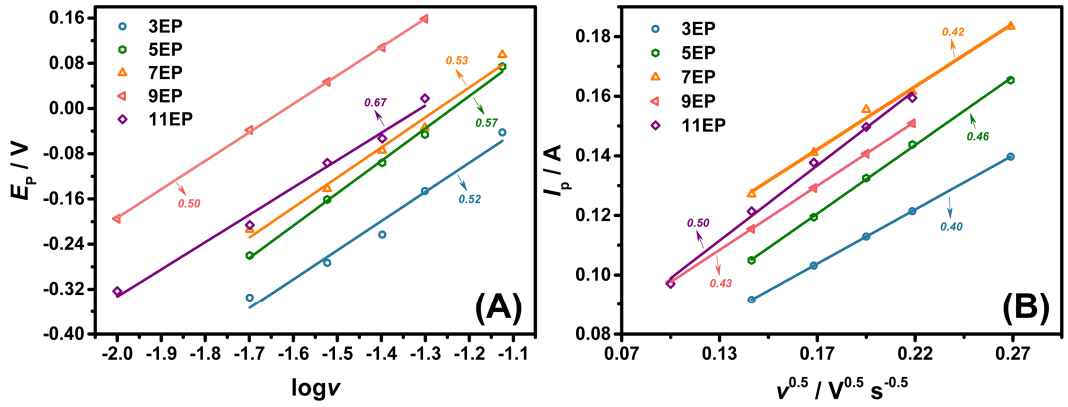

Fig. S6 (A) the dependence of peak current I_p on the square root of scan rate ($v^{1/2}$) and (B) the dependence of peak potential E_p on the logarithm of scan rate (log$v$)

Determination of heterogeneous rate constants (k_s)

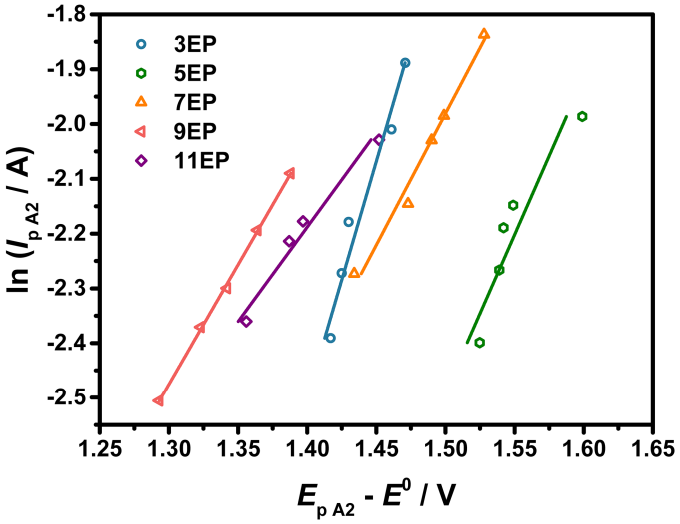

Fig. S7 Plots of ln $I_{p\,A2}$ vs. ($E_{p\,A2} - E^0$) of CoB/Ni-foam catalysts with different electroless plating times in N_2-saturated 0.05 mol L^{-1} $NaBH_4$ + 3 mol L^{-1} NaOH solution at 298 K

The standard heterogeneous rate constants k_s / cm s^{-1} during borohydride electrooxidation process could be calculated by the following equation [2]:

$$I_p = 0.227nFAc_{BH_4^-}k_s \exp\left\{\left[\frac{(1-\alpha)n_\alpha F}{RT}\right]\left(E_p - E^0\right)\right\}$$

where I_p was the peak current (A), n was the number of electron transferred (calculated in section 3.2), F was the Faraday constant (96485 C mol^{-1}), A was the active surface area (cm^2), C_R was the concentration of BH_4^- (mol dm^{-3}), E_p was the peak potential (V) and E^0 was the formal potential (V). The standard heterogeneous rate constants k_s could be obtained by plotting ln $I_{p\,A2}$ vs. ($E_{p\,A2} - E^0$) curves, and the intercepts of the curves was proportional to k_s. The results were summarized in Table S2.

Cell performance using CoB plate as anode

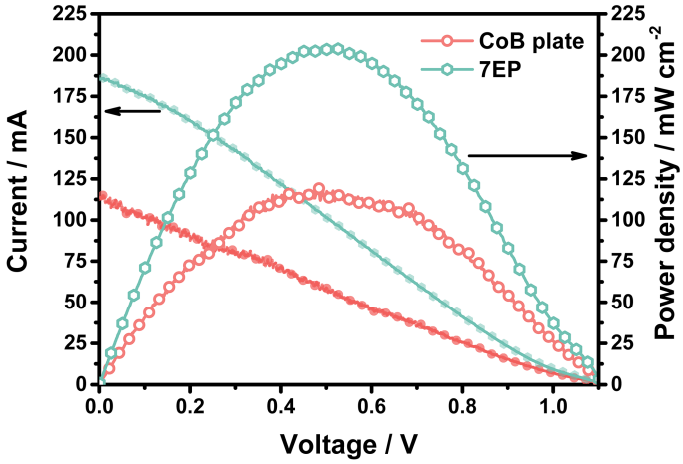

Fig. S8 Cell polarization and power density curves of the membraneless DBFC with CoB plate anode in 1 mol L^{-1} $NaBH_4$ + 3 mol L^{-1} NaOH solution at 303 K

Table. S1 The surface compositions and the corresponding binding energies of CoB/Ni-foam, CoB plate, Ag-sensitized Ni-foam

Catalyst		**5EP**	**7EP**	**11EP**	**CoB Plate**	**Ag-sensitized Ni-foam**
Surface composition (At. %)	Co	18.6	16.7	19.1	1.8	–
	B	6.6	8.1	10.9	0.7	–
	Ni	3.3	2.1	4.6	*	27.0
	Ag	0.04	0.05	0.06	–	–
	O	41.4	36.6	35.8	5.6	36.3
	C	30.0	36.4	29.4	29.7	36.7
	F	–	–	–	62.2	–
Binding energy / eV	Co^0	777.9	777.8	777.8	777.7	–
	B^0	187.9	187.9	187.9	187.4	–
	Ni^0	852.3	852.1	852.2	–	852.4

* The surface Ni content could not be obtained because the Ni 2*p* band of CoB plate was overlapped with F auger band and the Ni 3*p* band was too weak to be used for quantification.

Table. S2 Standard heterogeneous rate constants k_s / cm s^{-1} calculated from the plots of ln $I_{p\,A2}$ vs. ($E_{p\,A2} - E^0$)

Catalyst	3EP	5EP	7EP	9EP	11EP
k_s / cm s^{-1}	6.3×10^{-5}	6.9×10^{-5}	6.7×10^{-5}	6.3×10^{-5}	6.2×10^{-5}

References

1 Y. C. Lu, M. S. Chen and Y. W. Chen, *Int. J. Hydrogen Energy*, 2012, **37**, 4254-4258.

2 A. J. Bard and L. R. Faulkner, *Electrochemical Methods: Fundamentals and Applications*, John Wiley, New York, 4ed, 2001.

3 W. Xing, S. Z. Qiao, R. G. Ding, F. Li, G. Q. Lu, Z. F. Yan and H. M. Cheng, *Carbon*, 2006, **44**, 216-224.

4 C. H. Xu, B. H. Xu, Y. Gu, Z. G. Xiong, J. Sun and X. S. Zhao, *Energy Environ. Sci*., 2013, **6**, 1388-1414.

5 L. L. Zhang, R. Zhou and X. S. Zhao, *J. Mater. Chem*., 2010, **20**, 5983-5992.

6 C. B. Liu, H. Zhang, Y. H. Tang and S. L. Luo, *J. Mater. Chem. A*, 2014, **2**, 4580-4587.

7 N. Patel, R. Fernandes and A. Miotello, *J Catal*, 2010, **271**, 315-324.

8 C. Wu, Y. Bai, D. X. Liu, F. Wu, M. L. Pang and B. L. Yi, *Catal Today*, 2011, **170**, 33-39.

9 Y. Liu, Y. J. Wang, L. L. Xiao, D. W. Song, Y. P. Wang, L. F. Jiao and H. T. Yuan, *Electrochim. Acta*, 2008, **53**, 2265-2271.

10 Q. Zhu, D. S. Lu, J. J. Lin and L. Du, *J. Electroanal. Chem*., 2014, **722-723**, 102–109.

11 K. B. Wishvender and E. T. Jorge, *J. Electroanal. Chem*., 1971, **31**, 63-75.